Journal of
Synchrotron
Radiation

ISSN 1600-5775

Received 16 April 2013
Accepted 25 September 2013

Liquid X-ray scattering with a pink-spectrum undulator

S. Bratos,[a]* J.-Cl. Leicknam,[a] M. Wulff[b] and D. Khakhulin[b]

[a]Laboratoire de Physique Théorique de la Matière Condensée, Université Pierre et Marie Curie, 4 Place Jussieu, 75252 Paris, France, and [b]European Synchrotron Radiation Facility, BP 220, 38043 Grenoble Cedex, France. *E-mail: bratos@lptmc.jussieu.fr

X-ray scattering from a liquid using the spectrum from the undulator fundamental is examined as a function of the bandwidth of the spectrum. The synchrotron-generated X-ray spectrum from an undulator is 'pink', *i.e.* quasi-monochromatic but having a saw-tooth-shaped spectrum with a bandwidth from 1 to 15%. It is shown that features in $S(q)$ are slightly shifted and dampened compared with strictly monochromatic data. In return, the gain in intensity is 250–500 which makes pink beams very important for time-resolved experiments. The undulator spectrum is described by a single exponential with a low-energy tail. The tail shifts features in the scattering function towards high angles and generates a small reduction in amplitude. The theoretical conclusions are compared with experiments. The r-resolved Fourier transformed signals are discussed next. Passing from q- to r-space requires a sin-Fourier transform. The Warren convergence factor is introduced in this calculation to suppress oscillatory artifacts from the finite q_M in the data. It is shown that the deformation of r-resolved signals from the pink spectrum is small compared with that due to the Warren factor. The q-resolved and the r-resolved pink signals thus behave very differently.

Keywords: X-ray scattering; liquids; pink X-rays.

1. Introduction

The distortion of signals due to imperfect recording devices is omnipresent in experimental sciences. This is particularly well known in optical spectroscopy, where spectral lines are deformed by the finite slit width of the spectrometer. This deformation may be large enough to compromise the interpretation of the observed data. Similar problems are present in X-ray physics. Some of them are due to the finite duration of the probing X-ray pulses, and may be treated employing deconvolution techniques (Jansen, 1997). They were discussed in some detail in our recent paper, called in what follows Paper 1 (Bratos & Leicknam, 2012). Another imperfection is not only that the pulse duration may be too long but also that the raw synchrotron-generated X-ray spectrum is never strictly monochromatic; this holds true even for the fundamental emission line from an undulator which at modern synchrotrons has an asymmetric shape with a relative bandwidth of 1–15% (FWHM) peaked at E_M. Problems of this sort merit careful examination. A short review covering the field was published recently by Guerin *et al.* (2012). The perturbations of q-resolved signals were explored first by Haldrup *et al.* (2009). The incident beam was described as a superposition of a number of strictly monochromatic beams, and standard formulas were employed to calculate the corresponding signals. Superposing them then provides the final signal, which may be compared with experiment. This approach turned out to be relatively satisfactory, although some details escaped the analysis. The perturbation of r-resolved signals turned out to be much more difficult; it was studied very recently, both theoretically and experimentally (Lee *et al.*, 2013). Here, too, the incident X-ray beam was considered as a superposition of a number of monochromatic beams. It was then shown that the scattering data of a polychromatic beam remain a weighted sum of monochromatic data even in real space. It was next shown how, knowing the signal for a given value of r, for example $r = r_0$, all signals, whatever r, can be deduced from the signal calculated for $r = r_0$. This last signal was determined by attributing to it an arbitrary, but flexible, functional form with a sufficient number of adjustable parameters; the latter were fixed employing mean square optimization techniques. The difficulty with this method is its numerical accuracy, the effects under consideration being very small.

Although basically interested in time-dependent problems, we decided here to consider systems in thermal equilibrium. In fact, the distortion of signals due to the use of pink radiation is expected to be small when modern synchrotron X-ray sources are employed; it is thus most conveniently explored in the absence of perturbations, *i.e.* for systems in thermal equilibrium. It should be emphasized that the polychromatic

correction problem can be treated in a completely clean way. Once statistical properties of the noisy component of the incident X-ray radiation have been defined, the rest of the paper is free of any theoretical or computational approximation. Note finally that similar problems occur also with free-electron laser sources, due to the shot-to-shot fluctuations of recorded signals. The present study thus represents a contribution to the general theory of X-ray radiation.

2. Deformation of X-ray signals in *q*-space

As just stated, the system under consideration is a diluted liquid solution in thermal equilibrium. In principle the system is probed with monochromatic radiation. In reality the X-ray spectrum is pink, *i.e.* only quasi-monochromatic. At the European Synchrotron Radiation Facility, the spectral width $\Delta\lambda/\lambda$ of the U17 undulator used for fast time-resolved experiments is 3.5% (full width at half-maximum), but at other beamlines and synchrotrons the bandwidth can vary from 2 to 15% depending of the collimation of the electron beam. Our problem here is to explore the consequences of this deviation from an ideal monochromatic source. Our theory rests on the assumption that the undulator-generated pink X-ray wave is an incoherent superposition of fully monochromatic X-ray waves (Schotte *et al.*, 2002). The intensity distribution of the latter was found to be exponential: $I(E) = I_0 \exp[-\gamma'(E_M - E)]$ if $E < E_M$ and $I(E) = 0$ for $E > E_M$, where E_M is the cut-off energy and γ' is the bandwidth (Fig. 1). The relation between the FWHM, called ΔE_M, and γ' is defined by $\Delta E_M = \ln(2)/\gamma'$. The line-width comes from the Doppler-shifted off-axis radiation from the undulator collected in a finite-size aperture.

It is more convenient for the present purposes to replace E in the expression $I(E)$ by the quantity $q' = 4\pi/\lambda$. This variable q' has the dimensions of a wavevector but is proportional to the energy E. One finds easily

$$E = h\nu = h(c/\lambda) = (h/4\pi)c(4\pi/\lambda) = 1/2\hbar c q'. \qquad (1)$$

The relation between the quantity q' just introduced and the wavevector q of the theory of X-ray diffraction is $q = q' \sin\theta$.

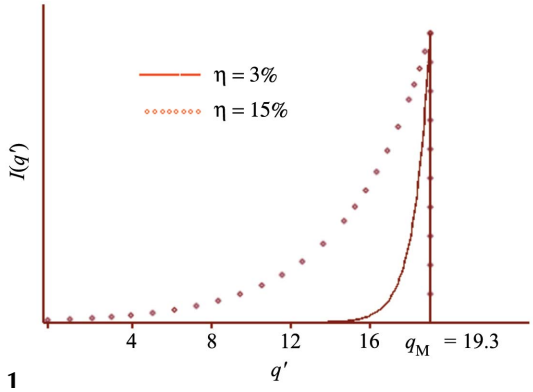

Figure 1
The shape of the synchrotron-generated X-ray intensity $I(q')$ as a function of the variable $q' = (4\pi/\lambda)$; this quantity is proportional to the beam energy E. Moreover, q_M is the cut-off value of q'. Note that E_M = 19 keV.

Expressing the energy E in terms of a quantity q' having the dimensions of inverse length may surprise, but note that in spectroscopy the energy is currently expressed in units of cm^{-1}. It is then possible to write $I(q') = I_0 \exp[-\gamma(q_M - q')]$ if $q' < q_M$, and $I(q') = 0$ if $q' > q_M$ where q_M is the cut-off value of q' and γ the bandwidth. As E and q' are proportional to each other, these two expressions are strictly equivalent. The decay constants γ and γ' are simply related, *i.e.* $\gamma = 1/2\hbar c\gamma'$. Then, if $S_P(\theta)$ is the intensity of the scattered pink radiation expressed in electronic units, 2θ the scattering angle and if $i_P(\theta) = S_P(\theta) - \Sigma_i f_i^2$ is its reduced scattering intensity from which the single atom contribution $\Sigma_i f_i^2$ was subtracted (Warren, 1990), there results

$$i_P(\theta) = \frac{\gamma}{1 - \exp(-\gamma q_M)} \int_0^{q_M} \exp\left[-\gamma(q_M - q')\right] i_M(q', \theta)\, dq' \quad (2)$$

where

$$i_M(q', \theta) = \sum_{i \neq j} f_i f_j \left\{\sin\left[q' r_{ij} \sin(\theta)\right] \Big/ q' r_{ij} \sin(\theta)\right\}.$$

Here, the symbol $i_M(q', \theta)$ indicates the reduced scattered X-ray intensity at a precisely defined value of q', q_M is the cut-off value of q' and f_i designates the atomic scattering factor of the atom i. The factor $\gamma[1 - \exp(-\gamma q_M)]^{-1}$ is the normalization factor for the undulator spectrum. Finally, the subscripts M and P refer to monochromatic and pink incident X-ray beams, respectively. This integral is not simply expressible in terms of familiar functions, but can easily be calculated numerically. Note that, if the incident X-ray radiation is not strictly monochromatic, the wavevector q is ill-defined, and speaking of q-resolved signals is not rigorous. On the contrary, the θ-dependent pink signals $S_P(\theta)$ remain precisely defined. Nevertheless, for commodity of language we will continue speaking about q-resolved signals, but one should keep in mind this precaution. This expression for the signal $i_P(\theta)$ can be used to explore the signal deformation if a pink, rather than a strictly monochromatic X-ray radiation, is used in an experiment. The two parameters playing a basic role here are the cut-off wave length vector q_M and the bandwidth $\eta = \Delta q_M/q_M = \Delta E_M/E_M$ of the X-ray spectrum. (i) The dependence of the q-resolved X-ray signal on the beam width η is illustrated in Figs. 2(*a*)–2(*c*). If q_M is of the order of 8 $Å^{-1}$ and $\eta \simeq 1\%$, the monochromatic and pink curves coincide. The X-ray radiation, although pink, can then be treated as monochromatic. If η increases to 3% with q_M = 8 $Å^{-1}$, the difference between the monochromatic and pink signals is no longer totally negligible. It is relatively important if $\eta \simeq 6\%$. Moreover, as shown in these figures, the nodal points of the pink signals shift more rapidly with increasing angle θ as in a monochromatic signal. Finally, the intensity of pink signals is smaller than that of monochromatic signals. These simple calculations give an idea about the effect of the polychromaticity of synchrotron-generated pink X-rays on q-resolved signals. These results are in good agreement with experiment (Guerin *et al.*, 2012; Haldrup *et al.*, 2009).

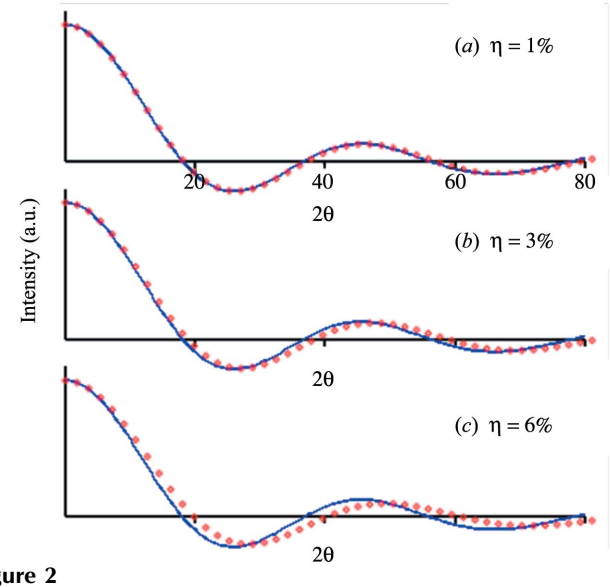

Figure 2
θ-resolved signals corresponding to different bandwidths of the incident X-ray beams (red squares). The blue curves represent signals generated by strictly monochromatic beams. The bandwidths are $\eta = 1\%$ in (*a*), 3% in (*b*) and 6% in (*c*).

The results can be understood using simple hand-waving arguments. In fact, let us consider a diatomic molecule of equilibrium length r_0 and replace the above distribution of wavevectors by two infinitely sharp lines placed at q_M and $q_M - 1/\gamma$; here $1/\gamma$ mimics the width of the real q' vector distribution. The resulting signals are $\sin(q_M r_0 \sin\theta)/(q_M r_0 \sin\theta)$ and $\sin[(q_M - 1/\gamma) r_0 \sin\theta]/[(q_M - 1/\gamma) r_0 \sin\theta]$. They vanish at $\sin\theta = n\pi/q_M r_0$ and $\sin\theta = n\pi/(q_M - 1/\gamma)r_0$, where $n = 1, 2, 3 \ldots$. It results that the signal corresponding to $\gamma \neq 0$ (the 'pink' signal) precedes the signal where $\gamma = \infty$ (the ideal monochromatic signal), and that this separation increases with increasing n. This is the essence of the results described above. Note, however, that the above conclusions must be refined if other perturbation mechanisms are active. For example, the signal-to-noise ratio of the measured signal may be affected by the asymmetric shape of the incident X-ray radiation. Unfortunately, studying these effects requires detailed knowledge of statistical properties of such perturbing mechanisms. This knowledge is rarely available at the present time.

The effects of pink X-rays have until now been studied theoretically. However, they can also be explored experimentally, symmetrizing the initially asymmetric undulator spectrum. A symmetric spectrum approaches the Dirac pulse $\delta(q - q_M)$, although it still remains pink. This result was obtained using specially constructed multilayer monochromators (Guerin *et al.*, 2012). A long-lasting effort was made at ESRF to realise satisfactory achievements. A first-generation multilayer monochromator was installed in the optics hutch in 2004. A double-crystal multilayer stage was attached to the cryogenic monochomator and was cooled by liquid nitrogen. This multilayer stage never worked well due to low-temperature stress from the Cu absorbers and vibrations in the cooling pipes that excited the second crystal. With the installation of the heat-load chopper in 2009, a modified multilayer stage, the in-focus multilayer monochromator, was installed 1.0 m from the sample. This stage is water-cooled. The performance is clearly superior due to the 1000 times lower heat load and the shorter distance to the sample. The first substrate is cooled by spring-loaded Cu absorbers. Both substrates have two coating stripes that can be moved into the beam. The first coating is a ruthenium coating with composition $[Ru/B_4C]_{51}$, giving a 3.2% bandwidth, and an iridium $[Ir/Al_2O_3]_{100}$ coating, generating a 1.6% bandwidth. The diffraction is dominated by the high-Z metals and the interlayer distances are 39.20 Å for Ru and 25.66 Å for Ir. The usable Bragg angles are 0.45–0.90° which gives 10–20 keV for Ru and 16–30 keV for Ir. Symmetric X-ray pulses obtained in this way are illustrated in Fig. 3, whereas one-pulse multilayer fluxes are shown in Table 1 which permits these fluxes to be compared with traditional silicium generated fluxes.

Table 1
One-pulse multilayer fluxes (photons pulse^{-1}).

15 keV (U17, harm 1)		25 keV (U20, harm 3)	
Pink, 5% bw	2.7×10^9	Pink beam	
Ru, 3.2% bw	4.3×10^8	Ir, 1.6% bw	3.3×10^7
Si(111), 0.014% bw	5.9×10^6	Si(111), 0.014% bw	8.1×10^5

3. Deformation of X-ray signals in *r*-space

This part of the present study refers to the r-resolved signals and is noticeably more complicated than that of the q-resolved signals. This problem has also been explored by other authors; see, for example, Lee *et al.* (2013). The following introductory remarks seem appropriate. Normally, the q-dependent signals $S(q)$ are measured experimentally using nearly monochromatic X-rays; structural information about the system can then be extracted by Fourier sine transforming them. The atom–atom distribution functions $g_{ij}(r)$ of the system can be

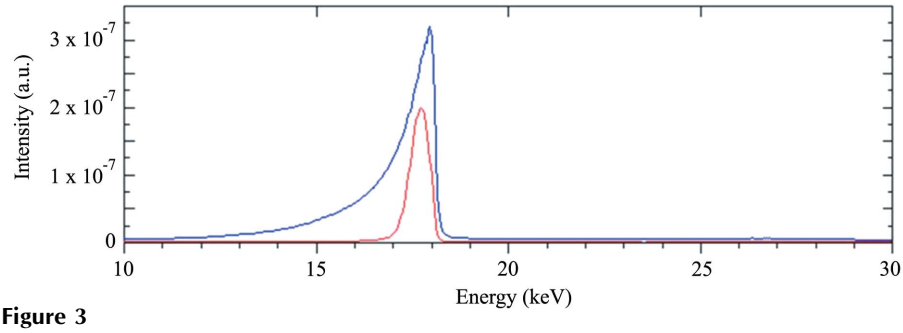

Figure 3
The blue curve shows the spectrum of the single-harmonic undulator measured with a Si monochromator. The red curve shows the spectrum monochromated by an Ir multilayer with a 1.6% bandwidth. In this figure the undulator beam intensity is expressed in terms of the energy E and not in terms of the variable q'.

obtained in this way. The purpose of the present study is different: it consists of investigating the effect of small changes of (supposedly known) atom–atom distribution functions $g_{ij}(r)$ on the scattered intensity. These changes may have a physical origin (*e.g.* thermal expansion of the system); they may also be introduced for mathematical convenience, for example the Warren correction (Warren, 1990). The basic equations for X-ray scattering from a liquid can then be written

$$\begin{aligned} i(q) &= S(q) - \sum_i f_i^2 \\ &= \sum_{i\neq j} f_i f_j \left\langle \exp\left(-iqr_{ij}\right)\right\rangle \\ &= \sum_{i\neq j} \left(f_i f_j / V\right) \int_0^\infty 4\pi r'^2 \left[g_{ij}(r') - 1\right] \frac{\sin(qr')}{qr'}\, \mathrm{d}r'. \end{aligned} \quad (3)$$

As earlier, $S(q)$ is the intensity of the scattered radiation expressed in electronic units, and $i(q)$ is its reduced form from which the single atom contribution was subtracted (Warren, 1990). Moreover, f_i is the scattering factor of the atom i, $g_{ij}(r')$ is the distribution function of the atoms i and j in a liquid solution and V is the volume of the liquid sample. Equation (3) by no means introduces a basic novelty into the theory of X-ray diffraction.

In the following we shall focus our attention on a diluted solution of diatomic molecules in an inert solvent. In fact, procedures exist to eliminate the solvent part of the experimentally measured signals (Cammarata *et al.*, 2006). What remains is a weighted sum of terms associated with the atom pairs AA, AB, AC, *etc.*, where A denotes the solute atoms and B, C, ... stand for solvent atoms. As these contributions usually peak in separate regions of the r-space, the signal of the AA pair can often be isolated. If this is the case, studying atoms A alone may suffice.

3.1. Warren correction

As the determination of $g_{ij}(r)$ invariably requires the Warren correction (Warren, 1990), the errors introduced by it are studied prior to the 'pink' effect. The main characteristics of this correction are as follows. The starting point is the observation that $i(q)$ approaches zero with increasing value of q due to the decrease in the values of $\sin(qr')/qr'$ with increasing q. At a maximum value in q, called in the following q_m, the quantity $i(q)$ becomes too small to be measured, and one can say that the intensity curve has converged. However, according to the basic theory of X-ray radiation (Warren, 1990), passing from q- to r-space requires a Fourier transformation of the function $qi(q)$ and not of the function $i(q)$ alone; this quantity may not be negligible even for the values of q larger than q_m, where $i(q)$ is no longer measurable. In addition, terminating $qi(q)$ at the highest value of q_m retained in this calculation produces false satellites. The Warren correction was invented (Warren, 1990) to overcome these difficulties and is of current use. It consists of introducing a convergence factor $\exp(-\alpha^2 q^2)$ and shifting the integration limit in q from ∞ to a limiting wavevector q_m in the Fourier transformation; this last step may be accomplished employing the step function $\Theta(x)$ equal to 1 if $x < 0$ and 0 if $x > 0$. Then introducing the usual normalization factor $M(q) = [\Sigma_{i\neq j} f_i(q) f_j(q)]^{-1}$, one can write

$$\begin{aligned} i_\mathrm{W}(r, q_\mathrm{m}) &= \frac{1}{2\pi^2 r} \int_0^\infty qM(q) i(q) \exp\left(-\alpha^2 q^2\right) \\ &\quad \times \Theta(q_\mathrm{m} - q) \sin(qr)\, \mathrm{d}q \\ &= \frac{1}{2\pi^2 rV} \sum_{i\neq j} \int_0^\infty 4\pi r' \left[g_{ij}(r') - 1\right] \mathrm{d}r' \\ &\quad \times \int_0^{q_\mathrm{m}} \left[f_i(q) f_j(q) \Big/ \sum_{i\neq j} f_i(q) f_j(q) \right] \\ &\quad \times \exp\left(-\alpha^2 q^2\right) \sin(qr) \sin(qr')\, \mathrm{d}q. \end{aligned} \quad (4)$$

This equation will now be simplified by neglecting the q-dependence of $f_i(q)$ and abbreviating $F_i = (\Sigma_{i\neq j} f_i f_j)^{-1/2}$. This simplification is introduced for reducing the following presentation to the essential physical dependence. In fact, we also performed calculations where this q-dependence of $f_i(q)$ was taken into account, but the resulting signals remain unchanged up to the precision of our calculations. Then, as $\sin(qr)\sin(qr') = (1/2)\cos[q(r - r')]$ if $(r + r')q \gg 1$, there results

$$\begin{aligned} i_\mathrm{W}(r, q_\mathrm{m}) &= \frac{1}{\pi rV} \sum_{i\neq j} F_i F_j \\ &\quad \times \int_0^\infty r' \left[g_{ij}(r') - 1\right] s_\mathrm{W}(r - r', q_\mathrm{m})\, \mathrm{d}r', \end{aligned} \quad (5a)$$

$$\begin{aligned} s_\mathrm{W}(r - r', q_\mathrm{m}) &= \int_0^{q_\mathrm{m}} \exp\left(-\alpha^2 q^2\right) \cos[q(r - r')]\, \mathrm{d}q \\ &= \left(\sqrt{\pi}/2\alpha\right) \exp\left[-(r - r')^2/4\alpha^2\right] \\ &\quad \times \mathrm{Re}\left\{ \mathrm{erf}\left[\left(2\alpha^2 q_\mathrm{m} - Ir + Ir'\right)/2\alpha\right]\right\}. \end{aligned} \quad (5b)$$

The error function entering in the above equation depends on a complex argument, I, indicating the imaginary unit. The intensity $i_\mathrm{W}(r, q_\mathrm{m})$, modified by the Warren correction, is given by the green curve in Fig. 5 whereas the blue curve in Figs. 4 and 5 indicates the 'true' signal written in the form $g_{AA}(r') - 1 = (1/V)\exp[-A(r' - r_0)^2]$, the distance r_0 being the equilibrium A–A distance. The deformation of the signal due to the Warren correction is seen to be very important. However, the maximum of the corrected signal is not shifted too much, which means that molecular geometry remains predicted correctly within this approximation. On the contrary, great care is necessary if this procedure is applied in studying molecular dynamics in liquids. Not only the position but also the shape of the signal plays a role in these circumstances.

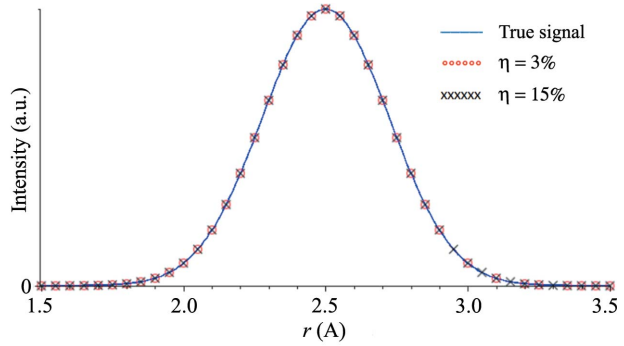

Figure 4
Comparing the *r*-resolved X-ray signals generated by monochromatic and pink incident X-ray beams. The blue line corresponds to a truly monochromatic beam, the red squares to a pink beam with bandwidth $\eta = 3\%$, and the black crosses to a pink beam with $\eta = 15\%$. Contrary to the *q*-resolved signals, the *r*-resolved signals are hardly affected by the polychromaticity of the incident X-ray beams. Compare with Fig. 2.

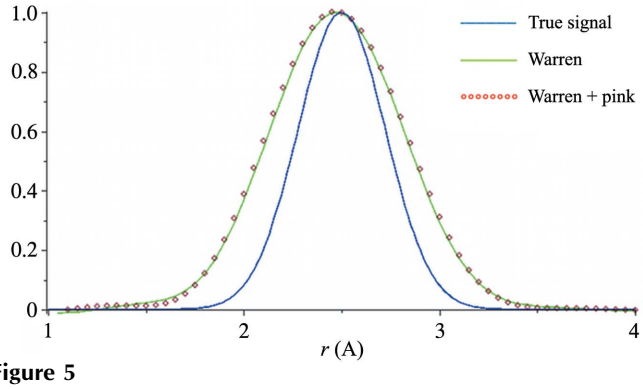

Figure 5
Comparing *r*-resolved signals generated by monochromatic and pink incident X-ray beams. The blue line corresponds to a truly monochromatic beam, the green line corresponds to the Warren deformed signal in the absence of polychromatic correction, whereas the red squares include both the effect of the Warren and that of the polychromatic correction. The perturbation of the signal due to the pink radiation is very small compared with that due to the Warren correction.

Another aspect of this problem also merits attention. As shown in equation (5), the deformed Warren signal $i_W(r,q')$ appears as a convolution of $\sum_{i\neq j}\{F_i F_j r'[g_{ij}(r')-1]\}$ with $s_W(r-r', q')$. It can thus be discussed in terms of the widely known convolution theory (Jansen, 1997). Convolution theory was initially employed in optics to describe the deformation of spectral shapes due to the finite slit width of spectrometers. It is extensively employed in treatments of images; compare with Paper 1 (Bratos & Leicknam, 2012) of this series. In convolution theory the convolution integral is generally written in the form $i(x) = \int dx' s(x-x')o(x')$, and the following terminology is widely adopted: the quantity $i(x)$ is called 'intensity', $s(x-x')$ is the 'point spread' or 'apparatus' function, whereas $o(x')$ is the 'object'. In spectroscopy, x, x' are frequencies, $i(x)$ is the observed band intensity at frequency x, $s(x-x')$ is the apparatus function and $o(x')$ is the true band intensity, free of any deformation. In X-ray diffraction, x and x' are interatomic *A*–*A* distances r and r', $i(x)$ is $i_W(r, q')$, s_W plays the role of the apparatus function, and $o(x') = \sum_{i\neq j}\{F_i F_j r'[g_{ij}(r')-1]\}$ is basically the weighted sum of non-deformed atom–atom distribution functions $g_{ij}(r') - 1$. These notions should be kept in mind to compare the deconvolution problems in spectroscopy and X-ray diffraction.

3.2. Pink signal in the *r*-space

Once the unavoidable jump over the Warren correction has been accomplished, we can return back to one of our main objectives, *i.e.* to the study of the pink X-ray signal $S_P(r)$, or of the reduced pink signal $i_P[r] = S[r] - \Sigma_i f_i^2$. This can be done by simply averaging the Warren signal i_W of equation (5) over the distribution of the limiting wavevectors q_m. Note that $q = q'\cos(\theta)$ and that $q_m = q'$. Then

$$i_P(r, q_M) = \frac{\gamma}{1-\exp(-\gamma q_M)}\int_0^{q_M}\exp\left[-\gamma(q_M - q')\right]s_W[q', r]\,dq'$$

$$= \frac{1}{\pi r V}\sum_{i\neq j}F_i F_j\int_0^{\infty} r'\left[g_{ij}(r')-1\right]s_P(r-r', q_M)\,dr'. \quad (6)$$

$$s_P(r-r', q_M) = \frac{\gamma}{1-\exp(-\gamma q_M)} \times \int_0^{q_M}\exp\left[-\gamma(q_M - q')\right]s_W[r-r', q']\,dq'. \quad (7)$$

The integrals present in (6) and (7) are all expressible in terms of elementary functions, mainly products of Gaussians and error functions of complex argument. Note that the expressions for $i_W(r,q')$ and $i_P(r,q_M)$ are both convolutions, differing from each other only in their apparatus functions $s_W(r-r',q')$ and $s_p(r-r',q_M)$.

The calculated signals $i_P[r,q_M]$ are reproduced in Figs. 4 and 5. (i) If the cut-off wavevector $q_M = 19.3\ A^{-1}$ and if the bandwidth of the pink beam is $\eta = 3\%$, the true signals and the pink signals, $i(r,q_M)$ and $i_p(r,q_M)$, coincide completely (Fig. 4). Note that current values of q_M attainable in practice are of the order of $10\ A^{-1}$; this figure thus describes conditions at which the undulator-emitted X-rays can be considered to be 'infinitely' sharp. (ii) The discussion is very different if the Warren expression $I(q)\exp(-\alpha^2 q^2)\Theta(q_M - q)$ is employed to pass from the *q*-resolved to the *r*-resolved signals (Fig. 5). In this case, the Warren correction covers largely the effects of pink X-ray radiation. This can be seen easily comparing the blue curve corresponding to the true signal, the green curve which is Warren corrected with $\alpha = 0.173$ A and $q_m = 8\ A^{-1}$, but where the X-ray radiation still is monochromatic, and the curve indicated by red squares where the radiation is pink, but the Warren parameters remain the same as above. The final parameters are $q_M = 8\ A^{-1}$, $\eta = 3\%$ and $\alpha = 0.173$ A. They are not arbitrary, but are inspired by those describing a dilute I_2/CCl_4 solution (Plech *et al.*, 2004). The smallness of the effect of pink radiation should not astonish. If the extension of the signal in the *r*-space is of the order of 1 Å, then, according to the relation $\Delta r\Delta q \simeq \pi$, the extension of the signal in the *q*-space is of the order 3 $Å^{-1}$. It is then not essential to realise the Fourier inversion by integrating over q up to ∞, up to

8 Å^{-1} or up to $8(1 - 1/\gamma) \simeq 7$ Å^{-1}. Using pink rather than monochromatic X-rays thus generates small effects difficult to study in the *r*-space.

4. Conclusions

The following conclusions may be drawn from this work. In *q*-space the signals generated by pink X-rays differ distinctly from their monochromatic analogues. These perturbations, although fairly small, are detectable and can be studied using multilayer monochromators; they can also be calculated theoretically. This statement no longer holds true in *r*-space. The Warren correction needed to pass from the *q*-space to the *r*-space introduces errors which cover the pink beam effect almost completely. Studying these effects on *r*-resolved X-ray signals $i(r)$ thus remains difficult at the present time and requires the development of more accurate data analysis and new strategies when coming to the refinement of high-resolution structural features from X-ray scattering data.

References

Bratos, S. & Leicknam, J.-Cl. (2012). *Ukr. J. Phys.* **57**, 133–139.

Cammarata, M., Lorenc, M., Kim, T. K., Lee, J. H., Kong, Q. Y., Pontecorvo, E., Lo Russo, M., Schiró, G., Cupane, A., Wulff, M. & Ihee, H. (2006). *J. Chem. Phys.* **124**, 124504.

Guerin, L., Kong, Q., Khakhulin, D., Cammarata, M., Ihee, H. & Wulff, M. (2012). *Synchrotron Radiat. News*, **25**, 25.

Haldrup, K., Christensen, M., Cammarata, M., Kong, Q., Wulff, M. S., Mariager, O., Bechgaard, K., Freidenhaus, R., Hemt, N. & Nielsen, M. M. (2009). *Angew. Chem. Intl Ed. Engl.* **48**, 4180–4184.

Jansen, P. A. (1997). *Deconvolution of Images and Spectra.* San Diego: Academic Press.

Lee, J. H., Wulff, M., Bratos, S., Petersen, J., Guerin, L., Leicknam, J.-Cl., Cammarata, M., Kong, Q., Kim, J., Moller, K. & Ihee, H. (2013). *J. Am. Chem. Soc.* **135**, 3255–3261.

Plech, A., Wulff, M., Bratos, S., Mirloup, F., Vuilleumier, R., Schotte, F. & Anfinrud, Ph. (2004). *Phys. Rev. Lett.* **92**, 125505.

Schotte, F., Techert, S., Anfinrud, P., Srajer, V., Moffat, R. & Wulff, M. (2002). *Third-Generation Hard X-ray Synchrotron Radiation Sources: Source properties, Optics and Experimental Techniques.* New York: Wiley.

Warren, B. E. (1990). *X-ray Diffraction.* New York: Dover.